JGR Atmospheres

RESEARCH ARTICLE
10.1029/2020JD032530

# Analysis of Location Errors of the U.S. National Lightning Detection Network Using Lightning Strikes to Towers

**Yanan Zhu[1], Weitao Lyu[2], John Cramer[3], Vladimir Rakov[4], Phillip Bitzer[5], and Ziqin Ding[4]**

[1]Earth Systems Science Center, University of Alabama in Huntsville, Huntsville, AL, USA, [2]State Key Laboratory of Severe Weather, Chinese Academy of Meteorological Sciences, Beijing, China, [3]Vaisala, Tucson, AZ, USA, [4]Department of Electrical and Computer Engineering, University of Florida, Gainesville, FL, USA, [5]Department of Atmospheric Sciences, University of Alabama in Huntsville, Huntsville, AL, USA

**Abstract** The location accuracy of the U.S. National Lightning Detection Network (NLDN) has been evaluated using as ground-truth rocket-triggered lightning data or video records but only at a few specific locations. In this study, by using the NLDN data for the events attributable to lightning strikes to towers, the location error of the NLDN across the entire contiguous United States was evaluated for the first time. We found that, on average, the NLDN median location error reduced from 198 to 84 m after the 2013 NLDN upgrade. The location error at the periphery of the network is significantly larger than that in its interior. In the coastal regions, there is directional location bias toward the water. Simulation results suggest that the bias is related to the lengthening of field waveform front due to electromagnetic wave propagation over lossy ground coupled with the asymmetrical sensor configuration relative to the strike point (lack of offshore sensors).

**Key Points:**
- NLDN location errors were estimated for CONUS using NLDN-reported events that can be reasonably attributed to lightning strikes to towers
- After the 2013 upgrade, the median location error averaged over the interior of the network is 75 m versus 158 m for its periphery
- The directional location bias in coastal regions is related to propagation effects coupled with the lack of sensors over water

**Supporting Information:**
- Supporting Information S1

**Correspondence to:**
W. Lyu,
lyuwt@foxmail.com

**Citation:**
Zhu, Y., Lyu, W., Cramer, J., Rakov, V., Bitzer, P., & Ding, Z. (2020). Analysis of location errors of the U.S. National Lightning Detection Network using lightning strikes to towers. *Journal of Geophysical Research: Atmospheres*, *125*, e2020JD032530. https://doi.org/10.1029/2020JD032530

Received 30 JAN 2020
Accepted 15 APR 2020
Accepted article online 19 APR 2020



## 1. Introduction

The U.S. National Lightning Detection Network (NLDN) has more than 100 sensors deployed in the contiguous United States (CONUS) with a typical baseline of 300–350 km. The NLDN detects signals produced by impulsive lightning processes in the very low frequency/low-frequency range and locates them by using the time of arrival and magnetic direction finding techniques. For each lightning event, the NLDN reports the time of occurrence, location, event type (intracloud or cloud-to-ground [CG] discharge), polarity, peak current estimate, semimajor and semiminor axes of location confidence ellipse (also known as location error ellipse), and field waveshape parameters, including risetime and peak-to-zero time. An overview of the NLDN can be found in Orville (2008) and Cummins and Murphy (2009).

Lightning data from the NLDN are used in various applications, such as weather forecasting, air traffic control, warning for outdoor recreation, and scientific research. Knowledge of the performance characteristics of the NLDN is important for adequate interpretation of those data. The NLDN performance was tested in many studies at different locations, in which video records and rocket-triggered lightning measurements were used as ground-truth data. Biagi et al. (2007) used video camera records to study the performance characteristics of the NLDN in 2003–2004 in Southern Arizona, Oklahoma, and Texas. By analyzing the NLDN locations of subsequent strokes that remained in the same channel as the first stroke, the median location error of the NLDN was found to be 424 m in Arizona and 282 m in Texas-Oklahoma. From 2004 to 2010, Warner et al. (2012) obtained high-speed video records for 81 tower-initiated upward flashes containing 151 subsequent events (either subsequent stroke or initial continuous current pulse) in South Dakota. By comparing the NLDN-reported locations with the locations of towers, it was found that the median location error of NLDN was 209 m. Using rocket-triggered lightning data as ground-truth, the University of Florida lightning research group examined the NLDN performance characteristics in Florida during three periods, 2001–2003, 2004–2009, and 2004–2013, and the corresponding median location errors were found to be 600, 308, and 309 m (Jerauld et al., 2005; Mallick, Rakov, Hill, Ngin, Gamerota, Jordan, et al., 2014a, Mallick, Rakov, Hill, Ngin, Gamerota, Pilkey, et al., 2014b; Nag et al., 2011), respectively. Although the studies mentioned above provided estimated location accuracy of the NLDN at several locations, the location accuracy across the entire network is unknown. Since the location accuracy can be influenced by many factors such as terrain and network configuration around a given location, the previous estimates of location accuracy at specific locations may be not applicable to other locations.

The difficulty of accurately determining the arrival time of lightning-generated field pulses at individual sensors is the main limitation preventing the NLDN from getting more accurate locations. As summarized in Schulz and Diendorfer (2000), the timing errors come from (1) the elongation of signal propagation path over uneven terrains (Li et al., 2016, 2017; Peng et al., 2020), (2) field peak delay caused by preferential attenuation of higher-frequency component due to the propagation over lossy ground (Cooray et al., 2000; Cooray & Lundquist, 1983; Uman et al., 1976), and (3) inaccurate determination of the pulse onset time. Cummins et al. (2010) and Honma et al. (2013) showed that location accuracy can be greatly improved after applying the propagation correction and onset correction, respectively. It was claimed that the median location accuracy of the NLDN improved from about 300 to 150 m in the interior of the network after the upgrade that underwent in 2010–2013, in which the onset correction was applied (Nag et al., 2013, 2014). Using lightning strikes to towers, it was found that 15 of the 22 towers showed median location errors less than 100 m in 2013 after the upgrade, with all having median errors less than 250 m (Cramer & Cummins, 2014).

In this study, the location accuracy of the NLDN was examined by using NLDN-reported CG lightning data around 1,451 towers with heights ranging from 150 to 629 m across the CONUS. An automated algorithm was developed to identify CG event density enhancement due to towers and CG events that likely terminated on the towers. Directional NLDN location biases were found at the periphery of the network and their cause was investigated using simulations.

## 2. Data and Methodology

The dataset of towers used in this study was obtained from the Obstacle database of U.S. Federal Aviation Administration. For each tower, the height above ground, height above sea level, and coordinates are provided. We filtered the tower data set by two criteria: (1) the tower needs to be taller than 150 m and (2) the tower has no other towers within 2 km. In order to have good coverage of the CONUS, we then selected the tallest 50 (it could be less than 50 since some states have less than 50 qualified towers after applying the two criteria stated above) towers in each state from the filtered tower data set. In this way, a total of 1,451 towers was selected. The heights of the towers range from 150 to 629 m with an arithmetic mean of 239 m. The locations of the 1,451 towers are shown in Figure S1 in the supporting information. The number of towers for each state can be found in Table S1 in the supporting information. Given the location of a selected tower, the information of NLDN-detected CG events within a 2-km radius around the tower is used for the periods from 2006 to 2009 and from 2014 to 2017.

It is well known that tall towers are preferred targets for lightning strikes. Towers taller than 100 m or so experience both downward and upward strikes (e.g., Rakov & Uman, 2003, Chapters 4 and 6). The percentage of upward flashes becomes higher with increasing tower effective height (Eriksson & Meal, 1984). Downward flashes (initiated by downward leaders) contain one or more return strokes and may contain M-components, which are current surges superimposed on continuing currents following some of the return strokes (Rakov et al., 2001). About three quarters of upward flashes (initiated by upward extending leaders from the tower) do not contain return strokes, only the steady current, called initial continuous current, usually with superimposed pulses that are similar to M-components (Diendorfer et al., 2009, and references therein). All impulsive current components with amplitudes greater than a few kA are expected to be recorded by the NLDN. Most of the flashes transport negative charge to ground and are referred to as negative. There are also positive and bipolar flashes that are expected to constitute less than 10% of all the flashes. In this study, focused on location errors, we do not make any distinction between the different impulsive processes in CG lightning flashes or their polarity and refer to all of them as "CG events."

Using 20 years of NLDN CG flash data gridded with a resolution of 500 m, Kingfield et al. (2017) found that 99.8% of high-flash-density (≥100 CG flashes) grid cells were within 1 km of an antenna tower. Figure 1a gives a typical example of the spatial distribution of CG events around a tower in the present study. The locations of NLDN-reported CG events from 2006 to 2009 within 2 km of a 588-m tower are shown. The tower is at the center (0, 0) of the plot. The CG events are gridded into cells of $50 \times 50$ m$^2$, and the corresponding color-coded density plot is shown in Figure 1b. One can see the elevated-density area around the center relative to the surrounding dark blue area with roughly uniform "background" density. Since the distribution of timing error of the NLDN sensor was approximately Gaussian (Cummins et al., 1998), the density is usually maximum at the center of the elevated-density area and gradually decreases with increasing distance from

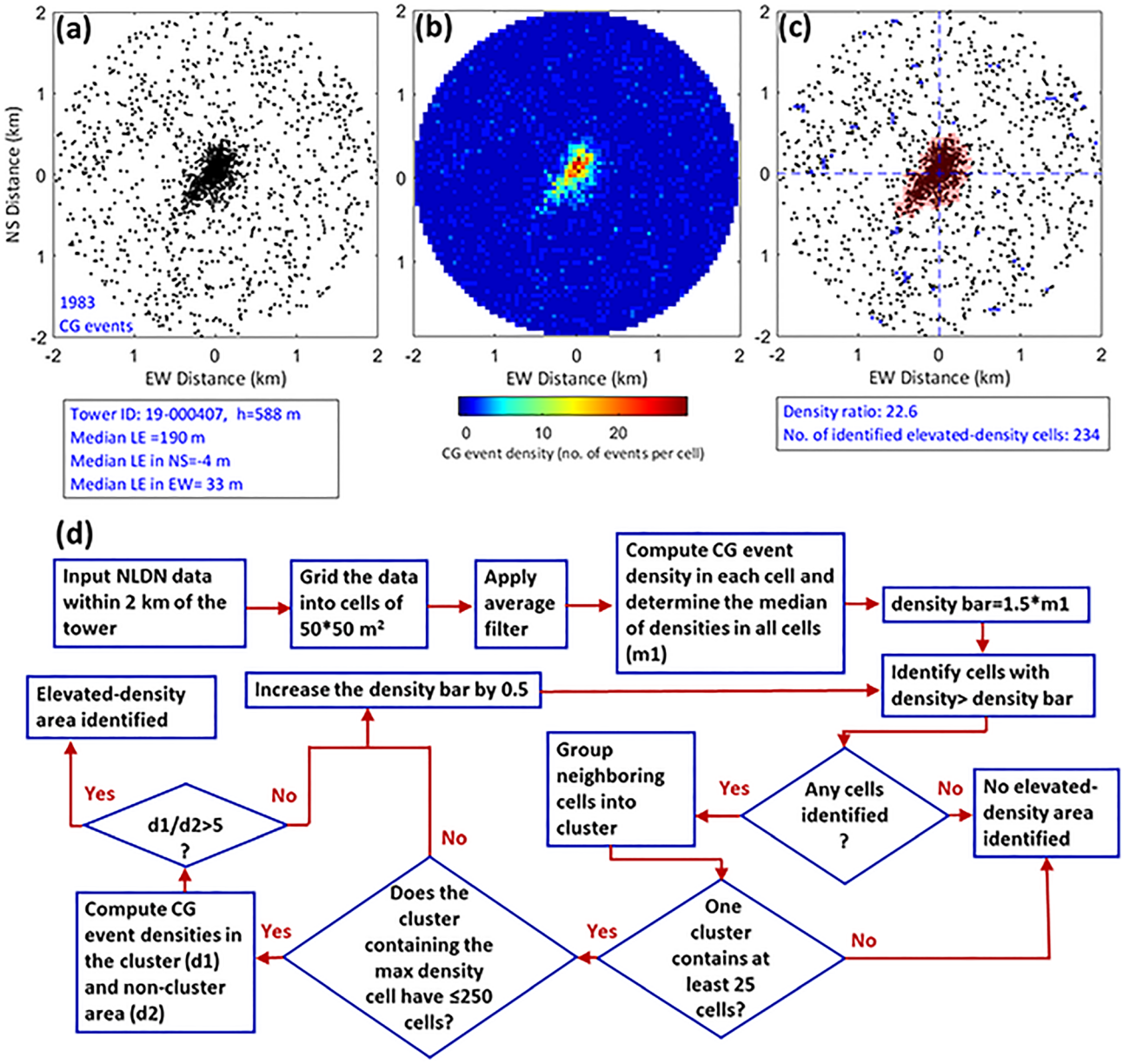


**Figure 1.** (a–c) Example and (d) flowchart to illustrate the algorithm used to identify the elevated-density areas of NLDN-reported CG events. LE stands for location error.

the center. The shape of the area with density enhancement is affected by the relative positions of nearby sensors.

The algorithm designed to identify elevated-density cells is shown in Figure 1d and described below. After the input of the NLDN-reported CG data within 2 km of the tower, we first gridded the data into cells of $50 \times 50$ m$^2$ and counted the number of CG events in each cell. Then we applied an averaging filter, which used the average number of CG events in a cell and its surrounding eight cells as the CG event density of the cell. This step served to reduce the irregular cell-to-cell variations. Specifically, it helped to remove single isolated cells with relatively high density. The median cell density $\times$ 1.5 was used as the initial density bar to search for elevated-density cells. If elevated-density cells were identified, we grouped the neighboring elevated-density cells into cluster(s) and only kept the cluster containing the cell with maximum density. If the cluster contained more than 25 cells, it was further checked if (1) the cluster contained less than 250 cells and (2) the ratio of densities in the cluster and noncluster area (see Figure 1c) was more than 5.

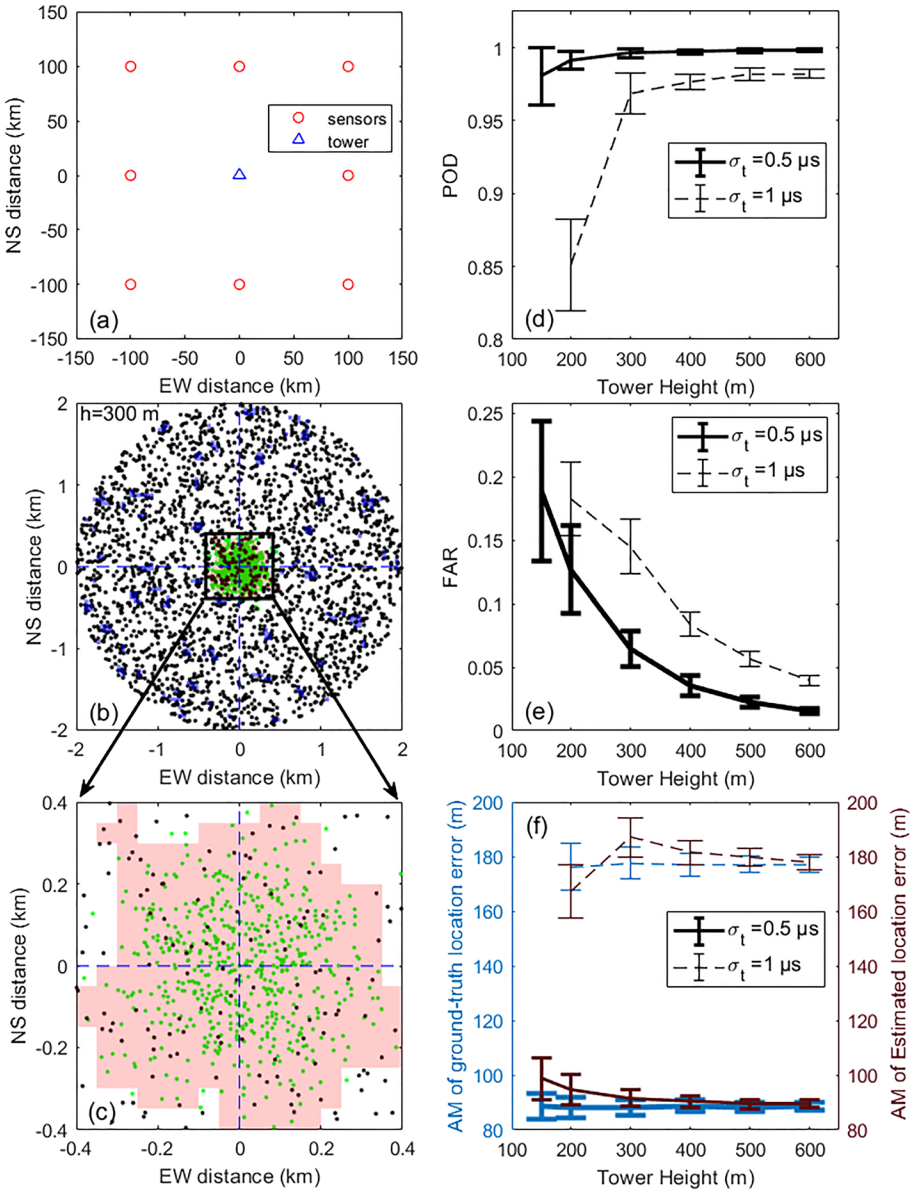


**Figure 2.** (a) The locations of tower and sensors in simulations. (b) An example of simulated CG event locations. Black and green dots are background and tower events, respectively. (c) Expansion of the square area in (b). The pink area is the elevated-density area detected by the algorithm. (d) Probability of detection (POD) versus tower height. (e) False alarm ratio (FAR) versus tower height and (f) simulated ground-truth median location error and median location error estimated by the algorithm for towers of different heights and for different timing errors ($\sigma_t$). The standard deviations are shown by vertical bars. Note that each data point in (c) and (d) is the arithmetic mean obtained from 100 simulations.

If yes, the cluster was accepted (labeled) as identified elevated-density area, otherwise, the density bar was increased by 0.5 and the searching/grouping process was repeated until either (a) a qualified elevated-density area was identified or (b) the algorithm failed to identify such an area. The criteria described above were set to make sure that (1) the tower does clearly show density enhancement around it, (2) the density bar is high enough to make the elevated-density area around the tower to stand out, and (3) the density bar is not too high so that only several cells of very high density that are very close to the tower stand out. In the example shown in Figure 1, the identified elevated-density area, containing 234 cells, is marked in red in Figure 1c. The ratio of the densities of the elevated-density area and the remaining background area is 22.6. Note that there are some scattered blue cells in Figure 1c; those are

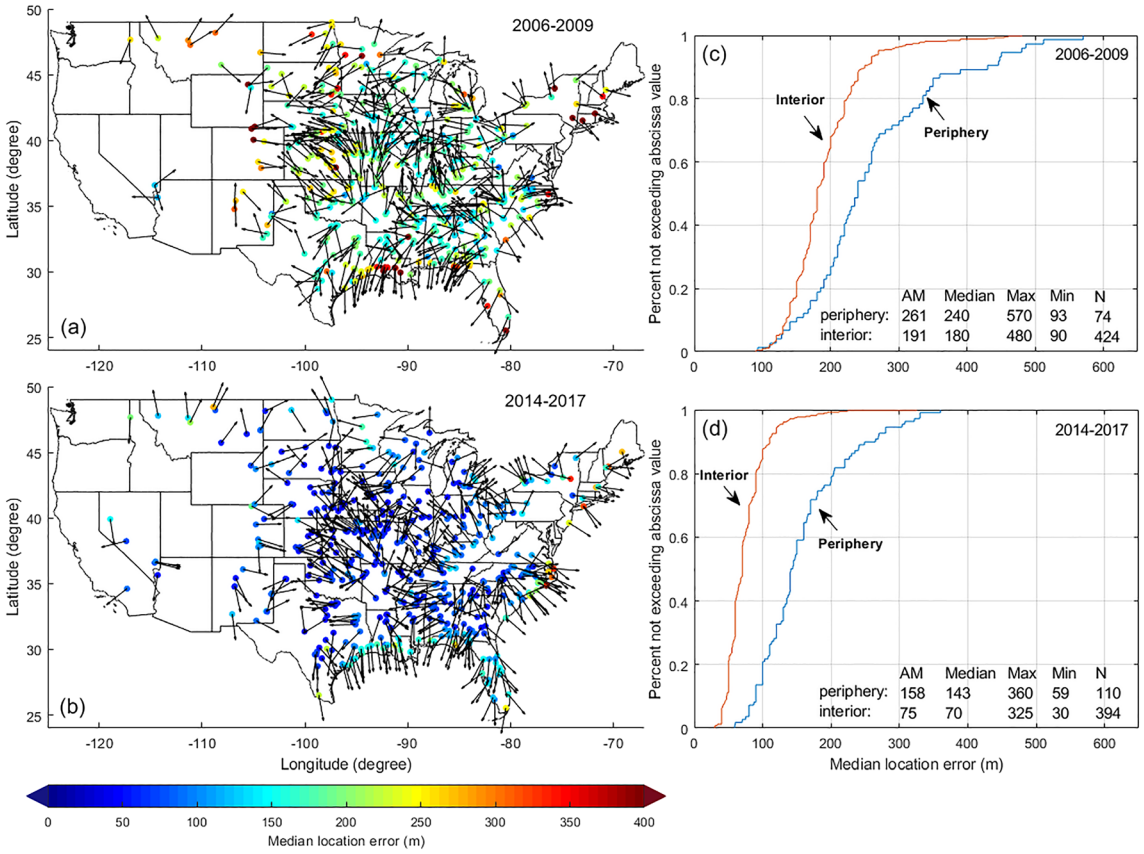


**Figure 3.** (a and b) Median location errors of the NLDN estimated using recorded lightning strikes attributable to tall towers for periods 2006–2009 and 2014–2017, respectively. Small circles represent positions of the towers, with the corresponding median location errors being color coded. The directional location biases are indicated by arrows. See also Figures 4a and 4b, which are the same as Figures 3a and 3b, but with location-bias arrows removed. (c and d) Cumulative median location error distributions in the peripheral and interior regions in the periods from 2006 to 2009 and from 2014 to 2017, respectively. Note that the number of towers investigated in both time periods is the same, while the number of data points in (a) and (b) is different, because the lightning incidence to a given tower does not always stand out above the background, in which case such tower cannot be used for estimating the location error.

cells with a density exceeding the density bar, but they could not be grouped into a cluster. All the CG events in the identified elevated-density cells are considered to be terminated on the tower whose location is known. Hence, location errors can be determined by calculating the distances from these events to the tower. The median location error estimated using this tower is 190 m. Besides the overall location error, we also computed the north-south and east-west components of location error, which are signed (positive for north and east and negative for south and west). The median location errors in north-south and east-west directions (directional biases) for this tower are -4 and +33 m, respectively.

The algorithm described above is able to identify most of the NLDN-reported CG events terminated on the tower. However, the inclusion of some nontower CG events terminated on the ground in the vicinity of the tower and the noninclusion of some tower events with very large location errors will introduce uncertainties in the estimated location error. In order to find out the uncertainties in the estimated location error, the locations of two types of CG events were simulated. The first type represents "background" CG events whose locations are uniformly distributed as if the tower were not present, and the second type represents events that terminated on the tower whose locations were simulated using a Monte Carlo simulation procedure (Koshak et al., 2004). Specifically, timing errors ($\Delta t_i$) that follow normal distribution were added to the ideal arrival times ($t_i$) at sensor $i$, and the "contaminated" arrival times ($t_i + \Delta t_i$) were sent into the nonlinear chi-square minimizer to produce the simulated locations of tower events. The location error associated with the magnetic direction finding was not considered in the simulation since the NLDN location error is primarily determined by errors in arrival times (Cummins et al., 2010). The configuration of sensors shown

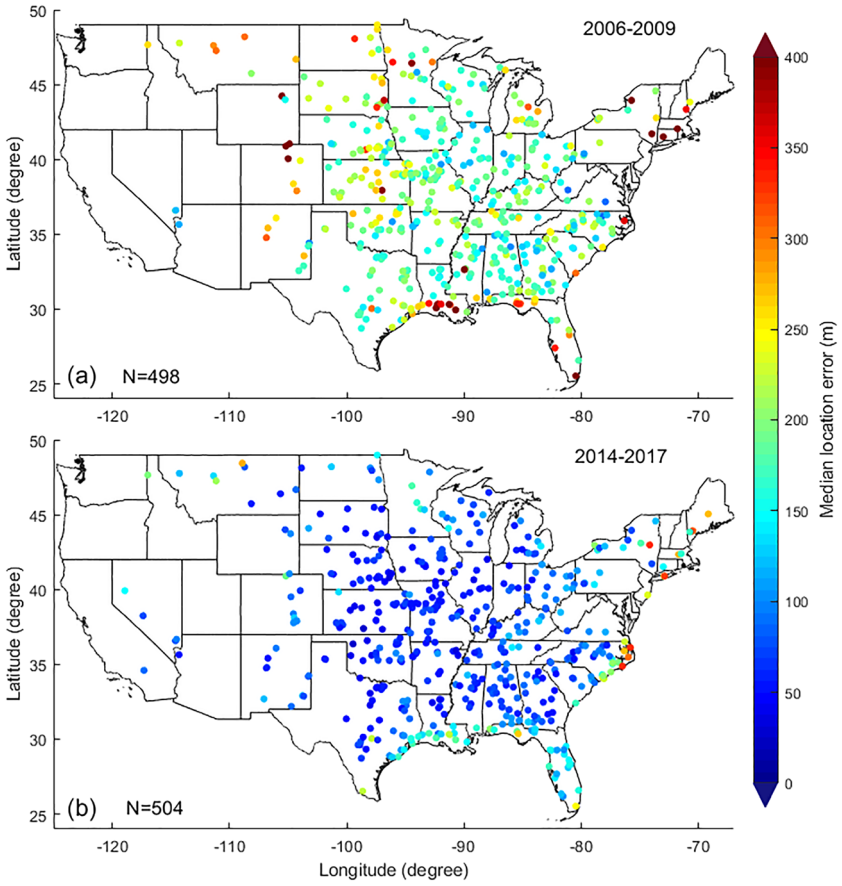


**Figure 4.** (a and b) Same as Figure 3a and 3b but with location-bias arrows removed.

in Figure 2a is used in the simulation. Note that the effect of tower attractive radius, which leads to a decrease in the number of "background" CG events with decreasing distance to the tower, is considered to be minimal and not taken into account in the simulation.

The number ($N_1$) of the first type of CG events (background events, assumed to be all associated with downward flashes) was calculated by using equation 1:

$$N_1 = N_g \times A \times T \times 4 \tag{1}$$

where $N_g$ is the ground-flash density, which is assumed to be 10 flashes per km$^2$/year in the simulation, $A$ is the area assumed in our analysis to be a circular area with a radius of 2 km (see Figure 1), and $T$ is the number of years that is assumed to be 4 because it corresponds to the time periods of NLDN data that we are going to investigate in the next section. The constant 4 in equation 1 represents the assumed average number of CG events per flash. The typical number of return strokes per flash is 3–5 for negative downward CG flashes (Rakov & Uman, 2003, Chapter 1). The number ($N_2$) of the second type of CG events (those terminated on towers, which may be associated with both downward and upward flashes) was calculated by using equation 2.

$$N_2 = \left(24 \times 10^{-6} h^{2.05} N_g\right) \times T \times 4 \tag{2}$$

where the expression in the parentheses, given by Eriksson (1987), is the estimate of annual lightning incidence (in flashes per year) to a tower of height $h$, which includes both downward and upward flashes. $N_g$, $T$, and 4 in equation 2 have the same meaning as in equation 1. We assume here that the number of NLDN-detectable impulsive processes in upward flashes is equal to 4. In Figure 2b, the simulated

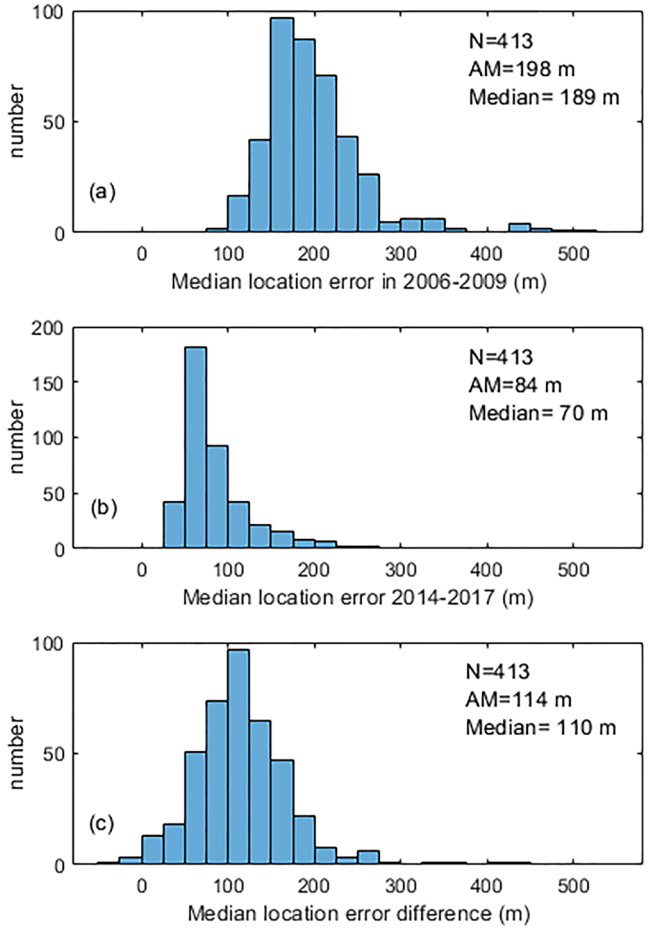


**Figure 5.** (a and b) Histograms of median location errors for 413 towers each with a detected elevated-density area both before (2006–2009) and after (2014–2017) the 2013 NLDN upgrade. (c) Histogram of the difference between the estimated median location errors before and after the 2013 NLDN upgrade. The arithmetic mean (AM) and median of abscissa values are given in each panel.

background events and events terminating on a 300-m tower are represented by black and green dots, respectively. The identified elevated-density area is marked in pink (see also the expansion shown in Figure 2c). One can also see in Figure 2b some scattered blue cells, which are cells with density above the threshold but not forming qualified clusters.

Simulations were performed for tower heights ($h$) of 150, 200, 300, 400, 500, and 600 m (covering the entire range of tower heights in this study) and root-mean-square timing errors of 500 ns and 1 μs. For each combination of tower height and timing error, simulations were performed 100 times with $N_1 + N_2$ events being passed through the algorithm presented in Figure 1. Because in the simulations we know which events were tower events and which events were nontower (background) ones, the arithmetic means and standard deviations of the probability of detection (POD), false alarm ratio (FAR), median ground-truth location error, and median estimated location error can be calculated. The results of these calculations are shown in Figures 2d–2f. The POD is the fraction of tower events that are correctly detected by the algorithm. The FAR is the fraction of algorithm-detected tower events that are actually background events. There are no data in Figures 2d–2d for the case of $\sigma_t = 1$ μs and $h = 150$ m, because the algorithm failed to identify an elevated-density area. This failure is due to the fact that the tower event density is not high enough to stand out of the background event density. Except for the case of $\sigma_t = 1$ μs and $h = 200$ m, the PODs for all other cases are above 95%. The FAR ranges from 2% to 18%. Taller objects and smaller timing errors are associated with a higher POD and a smaller FAR. Note that the FAR values are overestimated, since the actual number of background events should be smaller due to the presence of towers. The absolute differences between the Monte Carlo simulated ground-truth median location error and the median location error based on using the algorithm presented in Figure 1 range from 1 to 10 m, which are 1 to 2 orders of magnitude smaller than the actual location errors and suggest the median location error given by our algorithm can be used as a reasonable approximation to the real median location error.

## 3. Results

The NLDN location error was estimated using data in two 4-year periods, 2006–2009 and 2014–2017. These two periods were selected to see if and how the NLDN location accuracy changed due to the network upgrade conducted in 2010–2013. Out of the 1,451 towers selected, the algorithm presented in Figure 1 allowed us to identify lightning density enhancement in at least one of the two periods for 589 towers. Towers without detectable lightning density enhancement could result from various reasons, such as low overall lightning activity (i.e., western CONUS) and/or relatively low tower effective height (related to topography or/and presence of structures nearby). Another possible reason is the lack of upward flashes with impulsive current components. The estimated median location errors and location biases are shown in Figure 3, where each small circle represents a tower, the median location error for each tower is color coded, and the arrows indicate the direction of location bias. See also Figures 4a and 4b, which are the same as Figures 3a and 3b, but with location-bias arrows removed, to better visualize the colored circles. The direction of location bias is determined by the relative magnitudes of median location errors in the $x$ (EW) and $y$ (NS) directions. For example, if the median location errors in the x and y directions are −100 and 0 m, respectively, the bias arrow will point to the west. By comparing the color of circles in Figures 4a and 4b, one can see that the NLDN location accuracy improved after the 2010–2013 upgrade. Out of 413 towers with identified lightning enhancement in both periods, 408 showed a reduction in median location error ranging from 9 to 425 m. The histogram of the difference between the estimated median location errors before and after the

**Table 1**
*NLDN Location Errors Estimated for 40 States in the CONUS Using Lightning Strikes to Tower in 2014 to 2017 (After the 2013 Upgrade)*

| State | Number of towers | Arithmetic mean of median location errors (m)[a] | 95% confidence interval (m) | State | Number of towers | Arithmetic mean of median location errors (m)[a] | 95% confidence interval (m) |
|---|---|---|---|---|---|---|---|
| AL | 27 | 89 | (77, 101) | NC | 34 | 139 | (110, 168) |
| AR | 15 | 59 | (50, 67) | ND | 6 | 102 | (76, 129) |
| AZ | 1 | 50 | — | NE | 24 | 55 | (49, 61) |
| CA | 1 | 90 | — | NH | 0 | — | — |
| CO | 7 | 110 | (81,139) | NJ | 1 | 235 | — |
| CT | 1 | 145 | — | NM | 10 | 87 | (73, 101) |
| DE | 0 | — | — | NV | 5 | 99 | (74, 124) |
| FL | 23 | 146 | (129, 163) | NY | 15 | 160 | (119, 201) |
| GA | 23 | 76 | (66, 86) | OH | 17 | 91 | (82, 101) |
| IA | 17 | 63 | (56, 70) | OK | 18 | 64 | (55, 73) |
| ID | 1 | 195 | — | OR | 0 | — | — |
| IL | 13 | 59 | (53, 65) | PA | 5 | 112 | (89, 135) |
| IN | 5 | 67 | (52, 83) | RI | 0 | — | — |
| KS | 23 | 61 | (52, 70) | SC | 11 | 93 | (73, 112) |
| KY | 15 | 84 | (72, 96) | SD | 12 | 59 | (47, 71) |
| LA | 18 | 121 | (93, 149) | TN | 14 | 83 | (71, 95) |
| MA | 2 | 223 | (110, 335) | TX | 43 | 92 | (77, 107) |
| MD | 0 | — | — | UT | 0 | — | — |
| ME | 4 | 277 | (198, 355) | VA | 3 | 99 | (78, 119) |
| MI | 13 | 78 | (62, 94) | VT | 0 | — | — |
| MN | 6 | 135 | (101, 170) | WA | 0 | — | — |
| MO | 33 | 63 | (58, 67) | WI | 13 | 92 | (79, 105) |
| MS | 13 | 78 | (61, 96) | WV | 1 | 120 | — |
| MT | 8 | 131 | (77, 185) | WY | 3 | 93 | (80, 106) |

[a]In the case of multiple towers in a given state, the median location errors for all the towers are averaged over those towers and the 95% confidence intervals estimated. For eight states in the CONUS, no location errors could be estimated due to the lack of qualified towers.

upgrade is shown in Figure 5. The median location errors are 198 and 84 m (averaged over the 413 towers) for the periods 2006–2009 and 2014–2017, respectively.

For both periods, one can see in Figure 3 that, as expected, the NLDN location error is lower in the interior of the network and larger at its periphery (in the coastal regions and near borders), and this pattern is consistent with the modeled NLDN median location error over the CONUS (Nag et al., 2014, Figure 2). Figures 3c and 3d show the cumulative median location error distributions in the peripheral and interior regions for 2006 to 2009 and for 2014 to 2017, where the peripheral and interior regions are defined here, respectively, as the regions within and beyond the line (not shown in the figure) drawn 100 km of the U.S. border or its coastal line. For both periods, the distributions for the peripheral and interior regions are different at 1% significance level based on using the two-sample $t$ test. The arithmetic means are 261 m (periphery) versus 191 m (interior) for the period from 2006 to 2009 and 158 m (periphery) versus 75 m (interior) after the upgrade. Based on our results, the NLDN location errors (about 300 m between 2004 and 2013) estimated using rocket-triggered lightning in Florida (peripheral region) are not representative of the entire network and are higher than those for interior regions.

It is worth noting that the 163-m-tall tower labeled Tower 1 in the study of Warner et al. (2012) is also included in our database. The NLDN median location error estimated for this tower in our study is 230 m for the period from 2006 to 2009, which is not far from 206 m given by Warner et al. (2012) based on observations of upward lightning from 10 towers in Rapid City, South Dakota, from 2004 to 2010. This similarity gives us confidence that our algorithm is capable of dealing with upward flashes, which is the dominant type of lightning discharges to tall towers.

In Table 1, we present NLDN location errors estimated for 40 states in the CONUS using lightning strikes to towers in 2014–2017 (after the 2013 NLDN upgrade).

In the following, we examine the reason for locations being biased toward the water (away from the network) on the east coast and the coast of the Gulf of Mexico. The Monte Carlo simulation procedure introduced in section 3 was used again. The approximate NLDN sensor configuration in the southeast region

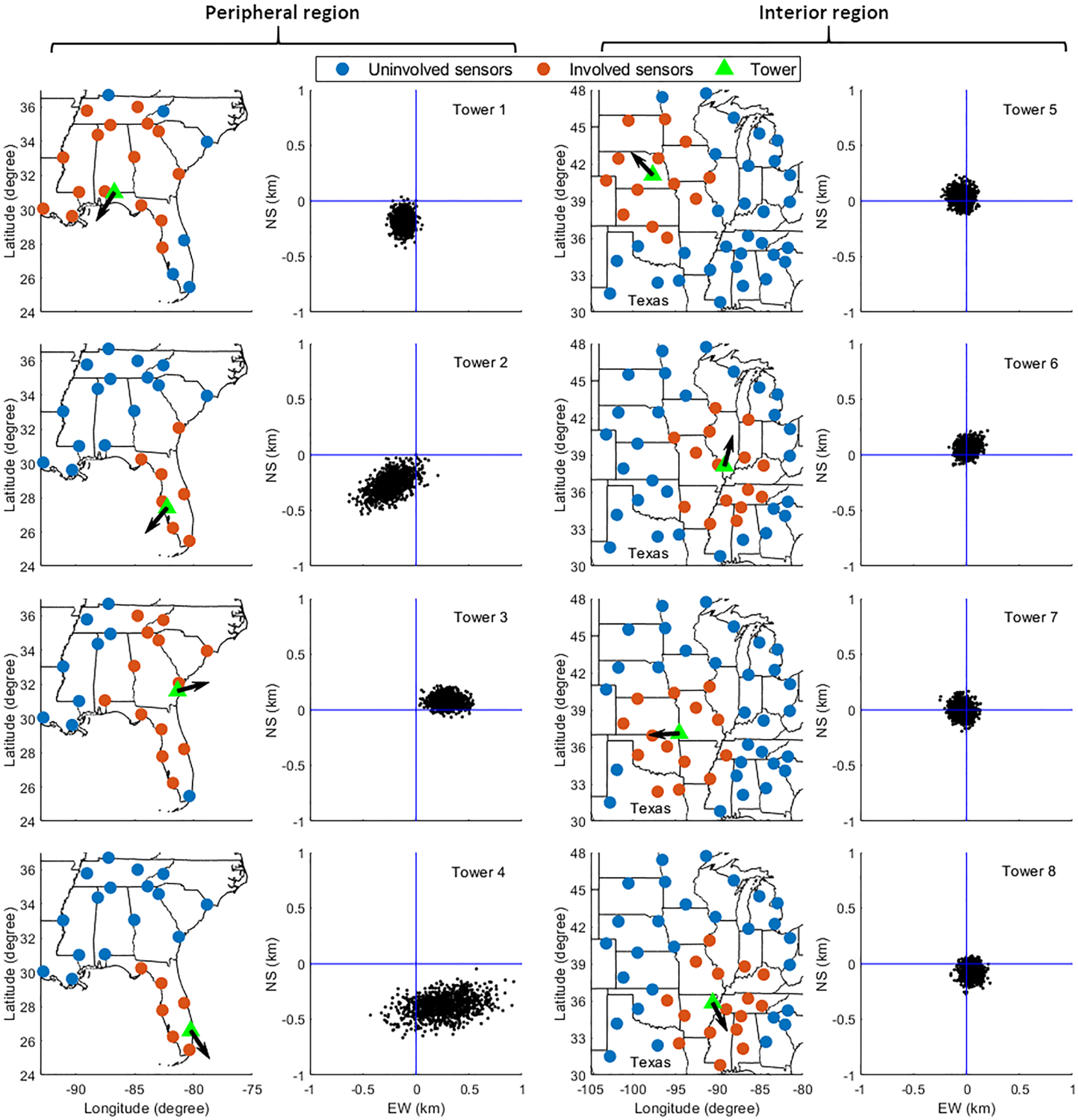


**Figure 6.** Panels in the first column show the approximate locations of the NLDN sensors (red and blue circles) and four tower locations (green triangles) in a peripheral region (Florida and neighboring states). Only sensors within 600 km of the tower (red circles) were assumed to be involved in geolocation. Panels in the second column show the simulated locations of 1,000 CG events, whose location biases are indicated by black arrows in the first column panels. The locations of towers are at the origin. The same format is used for the third and fourth columns, in which the four selected towers are located in an interior region centered on the state of Missouri. Clearly, the directional location bias is stronger for peripheral regions compared to interior ones.

was used in this simulation. The information on NLDN sensor locations for the examined time period is proprietary, so in simulations, the approximate NLDN sensor locations were obtained from an NLDN history paper (Orville, 2008, Figure 11), which are probably not far from actual ones and should be acceptable for our simulation purpose. Only sensors within 600 km of a tower participated in geolocation. In some initial simulation attempts, in which a tower was set at the edge of the sensor network, we found that under the assumption that all timing errors follow a normal distribution with a mean of 0, the median location error in EW and NS was always close to 0 regardless of the standard deviation of the timing error. Increasing the standard deviation only caused the location error to be more spread around the actual location but did not lead to any noticeable location bias. However, we found that if some time delay (e.g., several microseconds) were additionally added to the arrival times for some remote sensors, the location bias would appear and tend to be away from the network center, similar to what is seen in the coastal regions in Figure 3. This situation is very likely to occur in reality. When the electromagnetic pulse produced by a return stroke propagates over the finitely conducting (lossy) ground, the ground acts like a low-pass filter. Stronger attenuation of higher-frequency components causes the lengthening of field waveform front, which translates to a delay in arrival time. For a given conductivity, the delay is roughly proportional to propagation distance (Cooray & Lundquist, 1983). Thus, a longer propagation path is expected to yield a larger arrival time delay. The propagation path of 200 km in Florida caused the 10% to 90% risetime of return-stroke electric field pulses to increase by ~1 μs (Uman et al., 1976). Additionally, it was shown that the peak of return-stroke pulses was delayed by an average of 1.8 μs over the 130-km propagation over the land with the conductivity of 3 mS/m (Honma et al., 1998). The general trend is that the larger arrival time delay is associated with lower ground conductivity of the terrain over which the electromagnetic wave propagates (Bardo et al., 2004; Cummins et al., 2005).

In order to take the propagation effects into account, we simply assume 1-μs time delay per 200-km propagation path for all regions, so that a longer distance from the tower to the sensor is associated with a larger arrival time delay. The arrival time delay is independent of ground-conductivity along the propagation path in our simplified assumption. On top of the arrival time delay, random timing errors following a normal distribution with zero mean and standard deviation of 500 ns were added. Two portions of timing errors taken together are effectively equivalent to random timing errors following a normal distribution with a mean that equals the distance-dependent arrival time delay and a standard deviation of 500 ns. Four towers (Tower 1–4) in the peripheral regions (along the Florida Atlantic coast and the coast of the Gulf of Mexico) and four towers (Towers 5–8) in the interior regions were selected for simulation and their locations are shown in Figure 6. The panels in the second and fourth columns in Figure 6 are simulated locations for 1,000 CG events for each tower. Clearly, the location bias for each of the four towers in the peripheral region is toward the water (indicated by black arrows), which is similar to our observations shown in Figure 3. In contrast, the four towers in the interior region have much smaller location biases. The effect of sensor configuration (their positions relative to the tower) can also be seen in Figure 6. If the involved sensors (orange circles) are more spread in NS direction than in the EW direction, the locations will be less dispersive (tighter) in the NS direction than in the EW direction (e.g., Towers 3 and 4).

Although the systematic location bias cannot be clearly seen on the west coast due to the fact that only one tower can be identified with CG event enhancement, the biases seen on the east coast and on the coast of the Gulf of Mexico in Figure 3 probably also exists on the west coast. Note that the northern border of the United States cannot be considered as the periphery of the NLDN because the sensors from the Canadian Lightning Detection Network are used along with the sensors in the NLDN for lightning location, although some trend to northward location bias can be seen in Figure 3. It is not clear what causes this northward location bias. Location bias in the interior of the network does not show a clear pattern, because lightning in the interior of the NLDN is recorded by sensors from roughly all directions, while lightning occurring at the periphery of the NLDN is mostly recorded by sensors from one side; the configuration of nearby sensors is asymmetrical. One way to think about this is that an arrival time delay is translated into an effectively longer propagation path from a lightning source to the sensor. As a result, each sensor effectively "pushes" the NLDN-estimated location beyond the actual one. If the tower is surrounded by sensors from all sides, the biases introduced by individual sensors will tend to be mutually compensated. If, on the other hand, there is a lack of sensors on one side, this will cause an uncompensated bias toward the area with a deficit of sensors.

## 4. Summary

The location error of the NLDN was estimated for NLDN-reported events that can be reasonably attributed to lightning strikes to towers in the CONUS. To identify CG events that terminated on towers, the lightning enhancements around towers were identified using an automated algorithm and all CG events in the elevated-density region were assumed to be terminated on towers. Simulations suggest that the median location error estimated using our algorithm can be viewed as a reasonable approximation to the real median location error. The location errors of the NLDN were estimated for two periods, 2006–2009 and 2014–2017, to see the changes in location accuracy resulting from the 2013 NLDN upgrade. It was found that, on average, the NLDN median location error decreased from 198 to 84 m after the upgrade. The location error at the periphery of the network is significantly larger than in the interior of the network. Additionally, we found that NLDN-reported locations were biased toward the water in the coastal regions. By assuming an additional distance-dependent arrival time delay at each sensor caused by propagation effects, the observed location biases in coastal regions were reproduced in simulations. This result suggests that the directional location bias is caused by the lengthening of field waveform front (due the electromagnetic wave propagation over the lossy ground) coupled with asymmetrical configuration of the NLDN sensors relative to the lightning strike location in the coastal regions (lack of offshore sensors).

**Acknowledgments**
This work was supported by the National Key Research and Development Program of China (Grant 2017YFC1501504), the National Natural Science Foundation of China (Grant 41775010), and NSF Grant AGS-1654576. The information on towers used in this study and location errors estimated for each tower before and after the 2013 upgrade can be found online (https://figshare.com/articles/NLDN_location_error_detemined_from_towers/12056052).

## References

Bardo, E. A., Cummins, K. L., & Brooks, W. A. (2004). Lightning current parameters derived from lightning location systems: What can we measure? In *18th International Lightning Detection Conference (ILDC)*. Helsinki, Finland.

Biagi, C. J., Cummins, K. L., Kehoe, K. E., & Krider, E. P. (2007). National Lightning Detection Network (NLDN) performance in southern Arizona, Texas, and Oklahoma in 2003–2004. *Journal of Geophysical Research*, *112*, D05208. https://doi.org/10.1029/2006JD007341

Cooray, V., Fernando, M., Sörensen, T., Götschl, T., & Pedersen, A. (2000). Propagation of lightning generated transient electromagnetic fields over finitely conducting ground. *Journal of Atmospheric and Solar-Terrestrial Physics*, *62*(7), 583–600. https://doi.org/10.1016/S1364-6826(00)00008-0

Cooray, V., & Lundquist, S. (1983). Effects of propagation on the rise times and the initial peaks of radiation fields from return strokes. *Radio Science*, *18*(3), 409–415. https://doi.org/10.1029/RS018i003p00409

Cramer, J. A., & Cummins, K. L. (2014). Evaluating location accuracy of lightning location networks using tall towers. In *International Lightning Detection Conference*. Tucson, Arizona, USA.

Cummins, K L, Cramer, J. A., Brooks, W. A., & Krider, E. P. (2005). On the effect osf land:sea and other earth surface discontinuities on LLS-inferred lightning parameters. In *VIII International Symposium on Lightning Protection* (pp. 1–6).

Cummins, K. L., Murphy, M. J., Cramer, J. A., Scheftic, W., Demetriades, N., & Nag, A. (2010). Location accuracy improvements using propagation corrections: A case study of the U.S. National Lightning Detection Network. In *International Lightning Detection Conference*. Orlando,Florida, USA.

Cummins, K. L., & Murphy, M. J. (2009). An overview of lightning locating systems: History, techniques, and data uses, with an in-depth look at the U.S. NLDN. *IEEE Transactions on Electromagnetic Compatibility*, *51*(3 PART 1), 499–518. https://doi.org/10.1109/TEMC.2009.2023450

Cummins, K. L., Murphy, M. J., Bardo, E. A., Hiscox, W. L., Pyle, R. B., & Pifer, A. E. (1998). A combined TOA/MDF technology upgrade of the US National Lightning Detection Network. *Journal of Geophysical Research*, *103*(D8), 9035–9044. https://doi.org/10.1029/98JD00153

Diendorfer, G., Pichler, H., & Mair, M. (2009). Some parameters of negative upwardinitiated lightning to the Gaisberg Tower (2000–2007). *IEEE Transactions on Electromagnetic Compatibility*, *51*(3), 443–452.

Eriksson, A. J. (1987). The incidence of lightning strikes to power lines. *IEEE Transactions on Power Delivery*, *2*(3), 859–870. https://doi.org/10.1109/TPWRD.1987.4308191

Eriksson, A. J., & Meal, D. V. (1984). Incidence of direct lightning strikes to structures and overhead lines. In *IEEE Conference Publications* (Vol. 236, pp. 67–71).

Honma, N., Suzuki, F., Miyake, Y., Ishii, M., & Hidayat, S. (1998). Propagation effect on field waveforms in relation to time-of-arrival technique in lightning location. *Journal of Geophysical Research*, *103*(D12), 14,141–14,145. https://doi.org/10.1029/97JD02625

Honma, N., Cummins, K. L., Murphy, M. J., Pifer, A. E., & Rogers, T. (2013). Improved lightning locations in the Tohoku region of Japan using propagation and waveform onset corrections. *IEEJ Transactions on Power and Energy*, *133*(2), 195–202. https://doi.org/10.1541/ieejpes.133.195

Jerauld, J., Rakov, V. A., Uman, M. A., Rambo, K. J., & Jordan, D. M. (2005). An evaluation of the performance characteristics of the U.S. National Lightning Detection Network in Florida using rocket-triggered lightning. *Journal of Geophysical Research*, *110*, D19106. https://doi.org/10.1029/2005JD005924

Kingfield, D. M., Calhoun, K. M., & de Beurs, K. M. (2017). Antenna structures and cloud-to-ground lightning location: 1995–2015. *Geophysical Research Letters*, *44*, 5203–5212. https://doi.org/10.1002/2017GL073449

Koshak, W. J., Solakiewicz, R. J., Blakeslee, R. J., Goodman, S. J., Christian, H. J., Hall, J. M., et al. (2004). North Alabama Lightning Mapping Array (LMA): VHF source retrieval algorithm and error analyses. *Journal of Atmospheric and Oceanic Technology*, *21*(4), 543–558. https://doi.org/10.1175/1520-0426(2004)021<0543:NALMAL>2.0.CO;2

Li, D., Azadifar, M., Rachidi, F., Rubinstein, M., Diendorfer, G., Sheshyekani, K., et al. (2016). Analysis of lightning electromagnetic field propagation in mountainous terrain and its effects on ToA-based lightning location systems. *Journal of Geophysical Research-Atmospheres*, *121*, 895–911. https://doi.org/10.1002/2015JD024234

Li, D., Rubinstein, M., Rachidi, F., Diendorfer, G., Schulz, W., & Lu, G. (2017). Location accuracy evaluation of ToA-based lightning location systems over mountainous terrain. *Journal of Geophysical Research-Atmospheres*, *122*, 11,760–11,775. https://doi.org/10.1002/2017JD027520

Mallick, S., Rakov, V. A., Ngin, T., Gamerota, W. R., Pikley, J. T., Hill, J. D., et al. (2014a). An update on the performance characteristics of the NLDN. *23rd* International Lightning Detection Conference/5th International Lightning Meteorology Conference, *119*(7), 1–9.

Mallick, S., Rakov, V. A., Hill, J. D., Ngin, T., Gamerota, W. R., Pilkey, J. T., et al. (2014b). Performance characteristics of the NLDN for return strokes and pulses superimposed on steady currents, based on rocket-triggered lightning data acquired in Florida in 2004–2012. *Journal of Geophysical Research-Atmospheres*, *119*, 3825–3856. https://doi.org/10.1002/2013JD021401

Nag, A., Mallick, S., Rakov, V. A., Howard, J. S., Biagi, C. J., Hill, J. D., et al. (2011). Evaluation of U.S. National Lightning Detection Network performance characteristics using rocket-triggered lightning data acquired in 2004–2009. *Journal of Geophysical Research*, *116*, D02123. https://doi.org/10.1029/2010JD014929

Nag, A., Murphy, M. J., Cummins, K. L., Pifer, A. E., & Cramer, J. A. (2013). Upgrade of the U. S. National Lightning Detection Network in 2013. In *Lightning Protection (XII SIPDA), 2013 International Symposium on* (pp. 80–84).

Nag, A., Murphy, M. J., Cummins, K. L., Pifer, A. E., & Cramer, J. A. (2014). Recent evolution of the U.S. National Lightning Detection Network. In *23nd International Lightning Detection Conference (ILDC)*. Tucson, Arizona, USA.

Orville, R. E. (2008). Development of the National Lightning Detection Network. *Bulletin of the American Meteorological Society*, *89*(2), 180–190. https://doi.org/10.1175/BAMS-89-2-180

Peng, X., Wang, L., Zhang, J., Chen, J., & Dai, B. (2020). The field shielding effect of mountain on the lightning electromagnetic field. *Journal of Electromagnetic Analysis and Applications*, *12*(02), 15–28. https://doi.org/10.4236/jemaa.2020.122003

Rakov, V. A., Crawford, D. E., Rambo, K. J., Schnetzer, G. H., Uman, M. A., & Thottappillil, R. (2001). M-component mode of charge transfer to ground in lightning discharges. *Journal of Geophysical Research*, *106*(D19), 22,817–22,831. https://doi.org/10.1029/2000JD000243

Rakov, V. A., & Uman, M. A. (2003). *Lightning: Physics and effects*. New York: Cambridge University Press.

Schulz, W., & Diendorfer, G. (2000). Evaluation of a lightning location algorithm using an elevation model. *25th International Conference on Lightning Protection (ICLP)*. Retrieved from https://www.aldis.at/fileadmin/user_upload/aldis/publication/2000/4_ICLP2000_Schulz.pdf

Uman, M. A., Swanberg, C. E., Tiller, J. A., Lin, Y. T., & Krider, E. P. (1976). Effects of 200 km propagation on Florida lightning return stroke electric fields. *Radio Science*, *11*(12), 985–990. https://doi.org/10.1029/RS011i012p00985

Warner, T. A., Cummins, K. L., & Orville, R. E. (2012). Upward lightning observations from towers in Rapid City, South Dakota and comparison with National Lightning Detection Network data, 2004-2010. *Journal of Geophysical Research*, *117*, D19109. https://doi.org/10.1029/2012JD018346